JOURNAL OF MAGNETIC RESONANCE **64**, 479–486 (1985)

Self-Diffusion NMR Imaging Using Stimulated Echoes

KLAUS-DIETMAR MERBOLDT, WOLFGANG HÄNICKE, AND JENS FRAHM

Max Planck Institut für biophysikalische Chemie, Postfach 2841, D-3400 Göttingen, Federal Republic of Germany

Received April 15, 1985

NMR imaging of molecular self-diffusion is demonstrated for the first time using stimulated-echo (STE) NMR signals. Stimulated-echo acquisition-mode (STEAM) imaging has been described in a preceding paper. It is based on a $90°$–t_1–$90°$–t_2–$90°$–t_3 rf excitation sequence and relies on the detection of the STE signal appearing at $t_3 = t_1$. By incorporating a pair of pulsed magnetic field gradients into the first and third intervals of the STEAM sequence, the effect of molecular self-diffusion on NMR images may be qualitatively demonstrated. A variation of the strength of the gradient pulses and/or the diffusion time, i.e., the length of the second interval, yields a series of diffusion weighted images which allows the calculation of a synthetical image solely displaying the self-diffusion coefficient. Experimental results on ^{1}H NMR images of phantoms are presented which clearly demonstrate the potential of diffusion imaging as a new tool in medical diagnosis as well as for nonmedical applications.

The importance of parameters such as spin density, relaxation times T_1 and T_2, chemical shifts, and flow phenomena in NMR imaging has been the subject of numerous investigations. However, there are only few contributions dealing with the influence of molecular diffusion, although the self-diffusion coefficient may provide useful information for physiological studies *in vivo* as well as for medical diagnosis. Recently, the self-diffusion coefficient of water has been determined by ^{1}H NMR measurements in plant cells (*1, 2*) and in animal tissues *in vitro* (*3–5*). It has also been reported that its value is altered by a factor of two between malignant and benign tissues (*6*). In NMR imaging diffusion effects are caused by the presence of magnetic field gradients required for spatial discrimination of the signals. In general, diffusional processes in inhomogeneous magnetic fields lead to an attenuation of echo intensities. In fact, diffusion complicates the evaluation of reliable T_2 values from a multiecho NMR imaging experiment (*7*). Preliminary attempts have been made to quantitize its influence on spin-echo (SE) NMR images by measuring the intensity ratio within images of phantoms which have been recorded with slice-selective gradients of different field strengths (*8*).

In this paper a new technique is described which allows a spatially resolved measurement of the molecular self-diffusion coefficient. It arises as a combination of the Stejskal–Tanner NMR diffusion measurement (*9*) with the recently developed stimulated-echo acquisition-mode (STEAM) imaging technique (*10*). Two self-refocusing "pulsed" field gradients are incorporated into the basic three-pulse STEAM imaging sequence. They may provide "diffusion contrast" or enable a quantitative evaluation

0022-2364/85 $3.00

of diffusion coefficients from a series of diffusion weighted images. Although conventional NMR diffusion measurements without spatial resolution (*9, 11*) might also be applicable to SE-NMR imaging, the use of stimulated-echo (STE) signals seems to be especially suitable for *in vivo* conditions (*12–14*). This is because magnetizations decay rather slowly with the spin–lattice relaxation time T_1 during the second interval of a STEAM imaging sequence. Hence, signal losses due to relaxation during a long diffusion time are much less important for stimulated echoes than for spin echoes decreasing with T_2.

METHODS

The most important NMR signals generated by a sequence of three rf pulses with flip angles unequal to 180° such as

$$90°\text{–}t_1\text{–}90°\text{–}t_2\text{–}90°\text{–}t_3(\text{STE}) \qquad [1]$$

are the spin echo at $t_2 = t_1$ and the stimulated echo at $t_3 = t_1$. Sequence [1] was first described by Hahn (*12*). Recently, appropriate modifications and further developments were found to be of considerable value for multipurpose NMR imaging (*10*). Here the technique is shown to allow the measurement of diffusion coefficients via the detection of the STE signal.

For most applications of stimulated-echo imaging sequences it is of particular importance that the transverse magnetization components excited by the initial rf pulse are (partially) transformed into longitudinal magnetizations by application of the second pulse. During the first interval t_1 the magnetization components precess with their individual resonance frequencies and thereby lose their phase coherence with the effective spin–spin relaxation time $T_{2\text{eff}}$. Assuming an equal distribution of spin moments in the $x'y'$ plane of the rotating frame of reference prior to the second pulse, exactly half of the entire magnetization, namely all vector components perpendicular to the phase of the second rf pulse, are flipped into the z direction. The resulting longitudinal magnetization components thereby retain their "phase memory" so that after application of a third "read" pulse these may regain phase coherence. In fact, after precession of a period of length t_1 a STE signal of the macroscopic transverse magnetization is observed. The formation of the STE signal is identical to the process which leads to a SE signal at a time t_1 after the second pulse. The SE signal refers to the second half of the total magnetization precessing during the first interval and represents those components which have been colinear with the phase of the second pulse and thus remained entirely unaffected.

Figure 1 demonstrates a modification of sequence [1] which allows the measurement of self-diffusion coefficients by application of two (rectangular) magnetic field gradients of length δ in the first and third interval (*13, 14*). The gradients should be self-refocusing, i.e., their integral values should be identical, to leave nondiffusing spins unaffected. Such spin moments precess with exactly the same frequency during the first and third interval. Diffusing spins are characterized by their spatial displacement within a certain diffusion time and thus will have different precession frequencies during t_1 and t_3. Accordingly, complete refocusing is no longer possible. The observable STE attenuation can be taken as a quantitative measure for the frequency changes which in the case

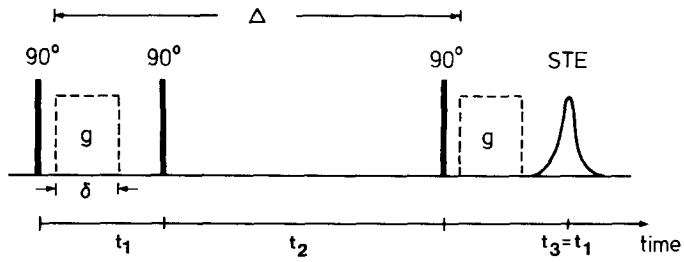

FIG. 1. Schematic diagram for the measurement of diffusion coefficients by means of stimulated echoes according to Ref. (*14*).

of linear field gradients directly refer to the spatial displacement by diffusional processes. Including relaxation effects the attenuation of the stimulated echo is given by (*14*)

$$\ln \frac{M}{M_0} = -\frac{t_2}{T_1} - 2\frac{t_1}{T_2} - \ln 2 - \gamma^2 D g^2 \delta^2 (\Delta - \delta/3) + K \qquad [2]$$

where M_0 refers to the initial amplitude of the NMR signal (i.e., the FID) and M denotes the actual amplitude of the STE signal. Further parameters are the diffusion time Δ between the two gradient pulses, the spin–lattice and spin–spin relaxation times T_1 and T_2, the molecular self-diffusion coefficient D, the gyromagnetic ratio γ, and the field strength g of the pulsed gradient. The constant K depends on the scalar product of the applied external gradient and the gradient of the internal field inhomogeneities and can be neglected under imaging conditions. By keeping the intervals t_1 and t_2 constant while varying the strength or the duration of the diffusion gradients in a number of experiments, it is possible to calculate the diffusion coefficient by means of a least-squares fit of the experimental data according to Eq. [2]. An alternative derivation of Eq. [2] assuming trapezoidal gradient pulse shapes modeling the real switching of gradients in a superconducting magnet results in only minor differences which may be neglected for experimental applications.

For imaging diffusion effects the modified STEAM imaging sequence shown in Fig. 2 will be appropriate. It is based on a previously described multislice STEAM imaging experiment (*10*) which allows the simultaneous recording of a number of directly neighbored slices. Since the magnetizations of the entire volume have been prepared by the two leading nonselective rf pulses, only the slice-selective readout pulse will be repeated with different irradiation frequencies to select magnetizations of individual slices. Each readout pulse thereby creates a corresponding slice-selective STE signal. The additional diffusion gradients may be applied in arbitrary directions in the first and third interval prior to acquisition of the STE. In Fig. 2 the diffusion gradient is chosen in the direction of the read gradient. The imaging sequence provides diffusion weighted images for a number of slices with the influence of diffusion becoming more important the higher the time integral of the gradient pulses.

In many biological systems as well as within a variety of nonliving materials the free diffusion of molecules such as water is limited due to the presence of cells or cavities. In principle, the diffusion STEAM imaging technique presented above should be able to distinguish between normal and restricted diffusion. This is because in the

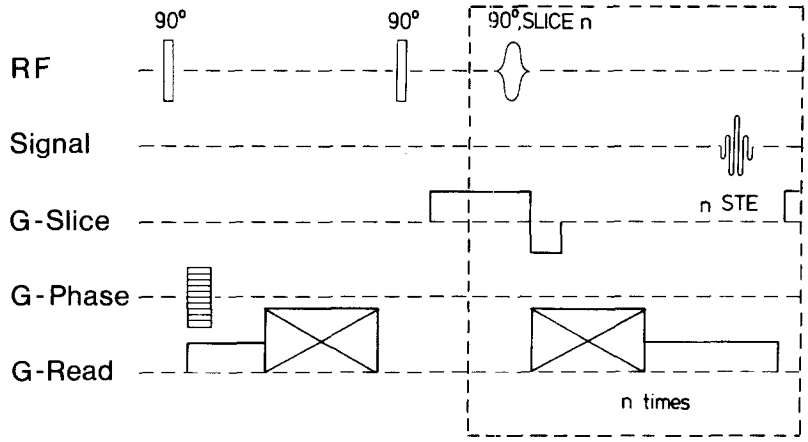

FIG. 2. Schematic rf pulse and gradient sequence for NMR imaging of diffusion effects using stimulated echoes (diffusion STEAM imaging). For multislice diffusion imaging the final read pulse is repeated with varying irradiation frequencies to select the desired planes.

case of restricted diffusion the observed diffusion coefficient becomes dependent on the diffusion time, i.e., the interval t_2. Two or more series of experiments with different values for t_2 therefore would allow a determination of the diffusion coefficient as a function of the diffusion time. However, since the STE intensity decreases with the spin–lattice relaxation time T_1 as t_2 is increased, the influence of restricted diffusion has to be discriminated against the influence of T_1. This can be easily done by means of another very efficient member of the STEAM imaging family which allows the simultaneous imaging of complete T_1 relaxation curves, i.e., ca. 20–30 images describing the T_1 decay, within the measuring time of a single conventional image with a repetition time of about $2T_1$ (*15*).

It should further be noted that all STEAM imaging sequences may be easily transformed into chemical-shift-selective (CHESS) imaging versions (*16*). For example, the initial rf pulse may be replaced by a frequency-selective pulse which, in the absence of a gradient, excites only a selected part of the entire NMR spectrum of the object under investigation. CHESS versions are not restricted to ^{1}H NMR imaging but in particular may deal with applications to heteronuclei such as fluorine or phosphorus exhibiting extended multiline NMR spectra. Finally, the diffusion STEAM sequence can be modified to allow spatially localized diffusion measurements. For this purpose all three rf pulses have to be used as "slice-selective" pulses with three perpendicular gradients. As a consequence the STE signal refers to a selected volume which may be easily varied in size, form, and location by varying the three gradient field strengths and/or the irradiation frequencies of the rf pulses, respectively. The diffusion measurement itself is performed in the same way as described above by recording the STE signal intensity as a function of field strength of the diffusion gradient.

RESULTS

Preliminary experimental demonstrations of diffusion imaging have been performed on phantoms using a combined imaging and spectroscopy system (Bruker BNT-100) with a 2.3 T superconducting magnet having a 40 cm bore. The substances under

investigation were aqueous solutions of 5×10^{-3} M copper sulfate and poly(ethyleneglycol) (PEG) with a molecular weight of about 6000–7500 and three water molecules per ethoxy group. Proton spin–lattice relaxation times T_1 of the compounds were determined at $T = 293$ K yielding $T_1(H_2O) = 430$ ms and $T_1(PEG) = 800$ and 250 ms for the two observed resonances (chemical-shift difference ca. 1 ppm, intensity ratio 2.5). Spin–spin relaxation times T_2 were measured to be $T_2(H_2O) = 400$ ms and $T_2(PEG) = 500$ and 200 ms, respectively.

First, diffusion coefficients have been determined without spatial resolution by means of the conventional Stejskal–Tanner SE-NMR technique but using the normal imaging gradient coils and power supplies to provide the pulsed diffusion gradients. Since the actual gradient field strengths have to be known for a quantitative evaluation of diffusion coefficients, they have been measured by recording frequency projections of a rectangular phantom with known dimensions. The evaluated diffusion coefficients are $D(H_2O) = 2.3 \times 10^{-5}$ cm^2 s^{-1} and $D(PEG) = 0.5 \times 10^{-5}$ cm^2 s^{-1} (293 K) in fair agreement with previous NMR measurements (*17, 18*). The range of diffusion coefficients covered by water and PEG corresponds to the range of water diffusion coefficients which may be expected in living tissues.

In a second step, prior to diffusion imaging, the normal image contrast of a phantom consisting of two tubes containing water and PEG has been investigated by application of a conventional STEAM imaging sequence with $t_1 = 30$ ms and $t_2 = 150$ ms. As shown in Fig. 3a no significant differences could be observed even when the repetition time T_R was varied from 0.5 s to 2.0 s. This finding has to be ascribed to the small differences of the mean T_1 and T_2 values. The sequence of images shown in Figs. 3b–d demonstrates the influence of an additional pair of diffusion gradients with increasing field strengths according to the imaging scheme of Fig. 2. The application of the diffusion gradients results in a dramatic increase of the contrast which is solely due to the different diffusion coefficients of water and PEG. The highest gradient strength was 7 mT m^{-1} and was switched on for a duration of 25 ms. The diffusion time Δ was 200 ms. Obviously, the use of conventional imaging gradients may already give an excellent visualization of diffusion effects within NMR images.

Beyond qualitative investigations of diffusion effects by recording images with and without a pair of diffusion gradients, it is further possible quantitatively to evaluate diffusion coefficients from a series of images recorded with different gradient field strengths. As demonstrated in Fig. 4, calculations according to Eq. [2] can be performed for each pixel independently yielding an image where intensities represent the diffusion coefficient. Figure 4a shows the calculated diffusion coefficient of an arbitrary pixel (marked by the cross) representing a volume element of size $1 \times 1 \times 4$ mm. An evaluation of the mean diffusion coefficient using region of interest (ROI) methods yields $D(H_2O) = (1.9 \pm 0.25) \times 10^{-5}$ cm^2 s^{-1} and $D(PEG) = (0.35 \pm 0.1) \times 10^{-5}$ cm^2 s^{-1}. Small deviations from the values without spatial resolution may be explained by the influence of the imaging gradients which are not negligible when using low diffusion gradients. A true parameter image is shown in Fig. 4b where calculated diffusion coefficients are encoded into an intensity scale. Only those values are displayed which could be fitted with a correlation factor greater than 0.9. In this image high intensities correspond to fast diffusion. In practice, color coding of diffusion coefficients turned out to be advantageous for a visualization of differences.

It should be noted that the limited gradient field strengths presently available in

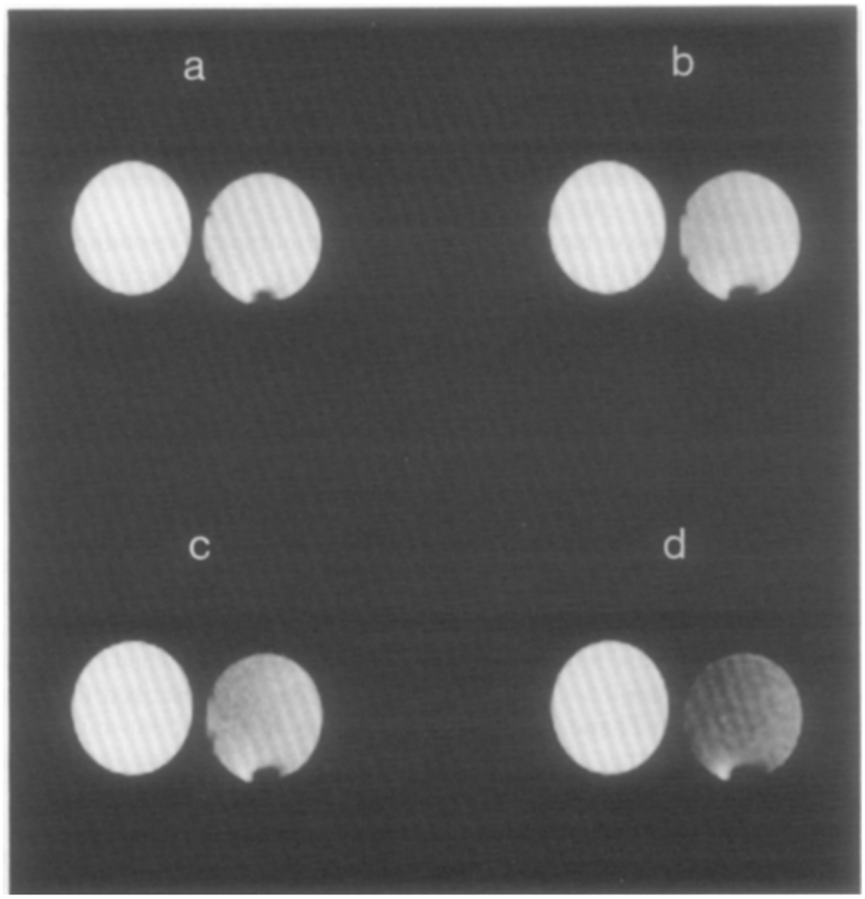

FIG. 3. Qualitative demonstration of diffusion effects according to the diffusion STEAM imaging sequence shown in Fig. 2 (n = 1). The images represent 100 MHz ^{1}H NMR images of a phantom comprising two tubes of an aqueous solution of $CuSO_4$ and poly(ethyleneglycol) (PEG), respectively. For each image 128 different phase-encoded projections have been recorded with a repetition time of 1 s leading to measuring times of about 2 min. The slice thickness was 4 mm, the intervals were t_1 = 30 ms, t_2 = 175 ms, and Δ = 200 ms. (a) STEAM image without application of a diffusion gradient. (b–d) STEAM images with diffusion gradients of field strengths increasing from 4 to 7 mT m^{-1}.

NMR imaging systems require rather long diffusion times, i.e., long durations of t_2. Although the magnetizations during this interval and hence the STE intensity decrease only with T_1, the signal-to-noise ratio of the resulting diffusion images may still be improved by shorter t_2 values. According to Eq. [2], the length of the t_2 interval may be reduced by a factor of four if the field strength of the diffusion gradient can be increased by a factor of two.

CONCLUSIONS

A new method for NMR diffusion imaging has been described which combines a STEAM imaging sequence and a diffusion measurement using pulsed gradients. Dif-

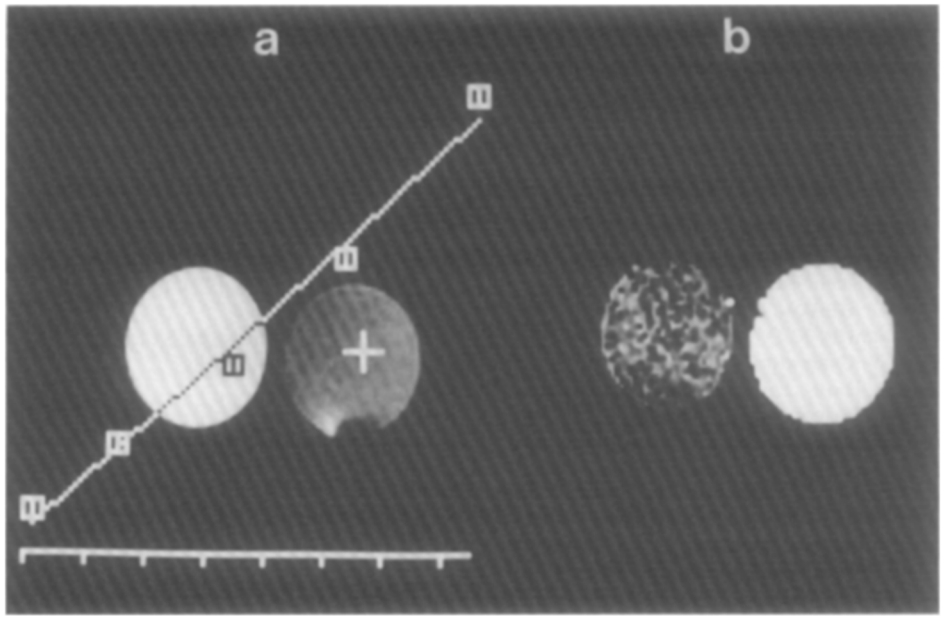

FIG. 4. Quantitative evaluation of diffusion coefficients from a series of five diffusion STEAM images (parameters as in Fig. 3). (a) Pixelwise computation of the diffusion coefficient. The diagram is a half-logarithmic plot of M/M_0 versus the square of the gradient field strength g (compare Eq. [2]). (b) True parameter image of the self-diffusion coefficient. Bright intensities correspond to high diffusion coefficients of the order of 2.5×10^{-5} cm^2 s^{-1}.

fusion contrast is imposed onto NMR images by means of a pair of self-refocusing gradients applied in addition to the imaging gradients. By varying the strength of the diffusion gradients, a series of images is obtained, which allows the calculation of spatially resolved diffusion coefficients, i.e., either values in selected regions of interest or even in the form of true parameter images. Since the use of STEAM imaging sequences is advantageous for systems with relaxation times $T_1 \gg T_2$, diffusion STEAM imaging should be especially promising for *in vivo* studies. Moreover, the new technique bears the principal potential for the imaging of restricted diffusion. Chemical-shift-selective (CHESS) variants will allow an extension to the imaging of heteronuclei with multiline spectra and thus, for example, may discriminate between diffusion coefficients of different fluorine- or phosphorus-carrying compounds.

ACKNOWLEDGMENT

Financial support by the Bundesminister für Forschung und Technologie (BMFT) of the Federal Republic of Germany is gratefully acknowledged (Grant 01 VF 242).

REFERENCES

1. J. E. TANNER AND E. O. STEJSKAL, *J. Chem. Phys.* **49,** 1768 (1968).
2. J. E. TANNER, *in* "Magnetic Resonance in Colloid and Interface Science," ACS Symposium, Series 34 (H. A. Resing and C. G. Wade, Eds.), p. 16, American Chemical Society, Washington D.C., 1976; D. G. STOUT AND R. M. COTTS, *in* "Magnetic Resonance in Colloid and Interface Science," ACS

Symposium, Series 34, (H. A. Resing and C. G. Wade, Eds.), p. 31, American Chemical Society, Washington D.C., 1976.
3. J. R. HANSEN, *Biophys. Acta* **230,** 482 (1971).
4. R. L. COOPER, D. B. CHANG, A. C. YOUNG, C. F. MARTIN, AND B. ANCKER-JOHNSON, *Biophys. J.* **14,** 161 (1974).
5. A. ANISIMOV, *Stud. Biophys.* **91,** 1 (1982).
6. C. F. HAZLEWOOD, G. CLEVELAND, AND D. MEDINA, *J. Natl. Cancer Inst.* **52,** 1849 (1974).
7. G. WESBEY, K. MOON, L. CROOKS, M. ARAKAWA, AND R. BRASCH, *Magn. Reson. Med.* **1,** 273 (1984) (Abstract).
8. G. WESBEY, M. MOSELEY, M. HROVAT, AND R. EHMAN, Third Annual Meeting of the Society of Magnetic Resonance in Medicine, New York, New York, August 13–17, 1984, p. 751.
9. E. O. STEJSKAL AND J. E. TANNER, *J. Chem. Phys.* **42,** 288 (1964).
10. J. FRAHM, K. D. MERBOLDT, W. HÄNICKE, AND A. HAASE, *J. Magn. Reson.* **64,** 81 (1985).
11. H. Y. CARR AND E. M. PURCELL, *Phys. Rev.* **94,** 630 (1954).
12. E. L. HAHN, *Phys. Rev.* **80,** 580 (1950).
13. D. E. WOESSNER, *J. Chem. Phys.* **34,** 2057 (1961).
14. J. E. TANNER, *J. Chem. Phys.* **52,** 2523 (1970).
15. A. HAASE AND J. FRAHM, *J. Magn. Reson.*, in press.
16. A. HAASE AND J. FRAHM, *J. Magn. Reson.* **64,** 94 (1985).
17. J. H. SIMPSON AND H. Y. CARR, *Phys. Rev.* **111,** 1201 (1958).
18. P. G. NILSSON AND B. LINDMAN, *J. Chem. Phys.* **87,** 4756 (1983).